# A Novel Approach to Simulating the Performance of Autonomous Inflow Control Devices

Ismail Hossain Rafi, Ali Moradi, Soheila Taghavi and Britt M. E. Moldestad



November 12, 2024

# A Novel Approach to Simulating the Performance of Autonomous Inflow Control Devices

**Ismail Hossain Rafi, Ali Moradi, Soheila Taghavi, Britt Margrethe Emilie Moldestad**

[1] *Department of Process, Energy and Environmental Technology, University of South-Eastern Norway, Norway.*

{ismailrafi16@gmail.com, ali.moradi@usn.no, soheila.t.hosnaroudi@usn.no, britt.moldestad@usn.no}

**Abstract**: Improving the efficiency of oil recovery is a crucial necessity in the current energy landscape. The widespread adoption of advanced wells, equipped with Autonomous Inflow Control Devices (AICDs), represents a leading strategy for this purpose. However, the absence of a predefined and straightforward option for modeling advanced wells in dynamic multiphase flow simulators like OLGA® poses a significant challenge. To address the issue, this paper proposes a novel approach based on developing a mathematical model derived from experimental data characterizing the AICD behavior. The Algebraic Controller option in OLGA is then leveraged to integrate the AICD effects into the simulation seamlessly. The proposed methodology undergoes rigorous testing on the PUNQ-S3 reservoir model as a benchmark case study with Water Alternating Gas (WAG) injection. Results demonstrate that AICD has a better water reduction rate of 36.3% and 3.7% compared to OPENHOLE and ICD. This result also indicates the accurate modeling and simulation of AICD performance in the software, showcasing the effectiveness of the developed mathematical model. Comparative analyses of advanced wells with different Flow Control Devices (FCDs) underscore the conclusion that AICDs significantly enhance oil recovery efficiency, thereby maximizing profit and minimizing the carbon footprint.

*Keywords*: OLGA, Near-well simulation, Advanced wells, AICD, Algebraic controller.

## 1. INTRODUCTION

Oil has been the most consumed energy among all the energy sources. Oil recovery has to be maximized considering the economic and environmental effects. Preventing early water and gas breakthroughs in horizontal wells is a major challenge in the oil industry. Inflow control technology like inflow control devices (ICD) and autonomous inflow control devices (AICD) were invented to minimize the issue of breakthroughs of unwanted fluid. AICD valve opening control is based on the properties of different fluids. Accurate modeling of the AICD behavior using a dynamic multiphase flow simulator like OLGA is important but challenging. Previous researchers tried to use the PID controller and Table controller to model the behavior of AICD. PID controller acts on a fixed setpoint, and Table controller is applicable for two-phase fluid mixtures like oil with gas or oil with water. Another approach is needed to consider the three-phase fluid mixture, a solution is to use the algebraic controller feature in the OLGA simulator. A logical or mathematical equation can be used as an expression form to control the valve opening output of AICD.

## 2. INFLOW CONTROL TECHNOLOGIES

### *2.1 Inflow Control Devices (ICD)*

ICD was invented in early 1990 by Norsk Hydro on the horizontal well section in the Troll field (Al-Khelaiwi and D.R., 2007). Due to reservoir heterogeneity, early water or gas breakthroughs can occur in the heel section or in high permeability zones. ICDs are mounted on the production tube as shown in Fig. 1. ICDs minimize the fluid flow with an additional pressure drop to create an even flow distribution along the horizontal well.

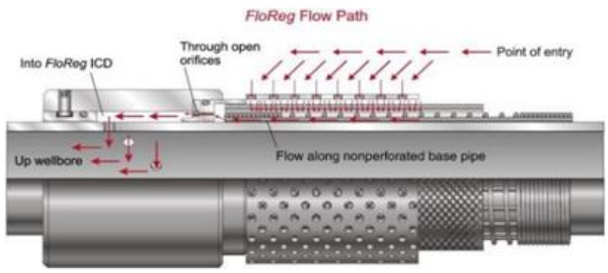


Figure 1: Orifice-type ICD setup and flow pattern of fluids (Birchenko et al., 2010).

However, ICD has a disadvantage as it cannot choke back the water after a breakthrough into the production pipe has occurred. For this reason, the water cut rises more than the capacity of the separation facilities can handle. The whole well needs to be choked to avoid this higher water cut. Choking the well results in minimizing oil production (Moradi and Moldestad, 2020). Many ICDs are mounted on a horizontal well. The pressure drop is the function of the flow rate, ICD geometry, and fluid density. In most cases, the orifice-type ICD is used, and the mathematical equation is:

$$\dot{Q} = C_D A \sqrt{\frac{2\Delta P}{\rho}}, \quad (1)$$

Where $\dot{Q}$ is the volumetric flow rate of the fluid through the ICD, $\Delta P$ is the pressure drop over the ICD, $\rho$ is the fluid density, $A$ is the cross-sectional area of the ICD nozzle, $C_D$ is the discharge coefficient.

*2.2 Autonomous Inflow Control Devices (AICD)*

An uneven production flow can still be observed from the toe to the heel section of a horizontal well even when using ICDs. This occurs due to frictional pressure drop and permeability variations in different regions. ICD can delay the breakthrough of unwanted fluids but cannot stop the breakthrough. Among all types of AICD, the AICD developed by Statoil is the most commonly used. A schematic of an RCP version of AICD is shown in Fig 2. AICD is functional with the viscosity differentials of the fluids. The RCP valve reduces the flow of low-viscous fluids like water and gas and is fully open for high-viscous fluids like oil (Mathiesen et al., 2011).

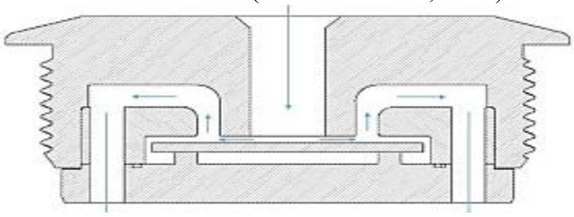

Figure 2: Schematic of the RCP valve developed by Statoil (Mathiesen et al., 2011).

Taking the function of fluid properties and volume flow empirical equation of differential pressure is:

$$\Delta P = f(\rho, \mu) \cdot a_{AICD} \cdot \dot{Q}^{x}, \quad (2)$$

$$f(\rho, \mu) = \left(\frac{\rho_{mix}^{2}}{\rho_{cal}}\right) \cdot \left(\frac{\mu_{cal}}{\mu_{mix}}\right)^{y}, \quad (3)$$

Where, $\dot{Q}$ is the volumetric flow rate of the fluid through the RCP, $\Delta P$ is the pressure drop over the AICD. $a_{AICD}$, $x$, and $y$ are the parameters specified by the user depending on the fluid properties and the RCP design criteria. $f(\rho, \mu)$ is the function of the density and viscosity in which $\rho_{cal}$ and $\mu_{cal}$ is the calibrated density and viscosity respectively. The equations for mixture density and viscosity are as follows:

$$\rho_{mix} = \alpha_{oil}\rho_{oil} + \alpha_{water}\rho_{water} + \alpha_{gas}, \quad (4)$$

$$\mu_{mix} = \alpha_{oil}\mu_{oil} + \alpha_{water}\mu_{water} + \alpha_{gas}\mu_{gas}, \quad (5)$$

Where $\alpha_{oil}$, $\alpha_{water}$, and $\alpha_{gas}$ is the volume fraction of oil, water, and gas in the mixture respectively.

## 3. PUNQ-S3 RESERVOIR MODEL

For this study, the PUNQ-S3 (Production forecasting with Uncertainty Quantification, variant 3) synthetic reservoir model is used and designed in ECLIPSE. Elf Exploration Production implemented this model in the real field according to the reservoir engineering study. It is a three-dimensional dome-shaped heterogeneous reservoir containing a total of 2660 grid blocks, of which 1761 blocks are active. The dimensions of the reservoir are given in Table 1. Corner point geometry and the Carter-Tracey aquifer were used to design this reservoir (Hutahaean, 2017). It has a Bottom Hole Pressure (BHP) of 220 bar with a maximum liquid production rate of 4000 $m^3$/day.

Table 1: PUNQ-S3 reservoir grid dimensions.

| **Direction** | **No. of blocks** | **Length (m)/dip angle** |
|---|---|---|
| x | 19 | 19×180 |
| y | 28 | 28×180 |
| z | 5 | 2355/1.5° |

The production well and the four injectors are designed by trial-and-error method for more oil production and to minimize early water and gas breakthroughs. Water and $CO_2$ are simultaneously injected by the four injectors at a regular time interval. Injectors 1, 2, 3, and 4 are placed at the depth of 2390 m, 2375 m, 2370 m, and 2370 m respectively. Fig. 3 represents the positioning of the injectors and production pipe with top face depth. The length of the horizontal well is 3240 m which is designed in the OLGA simulator.

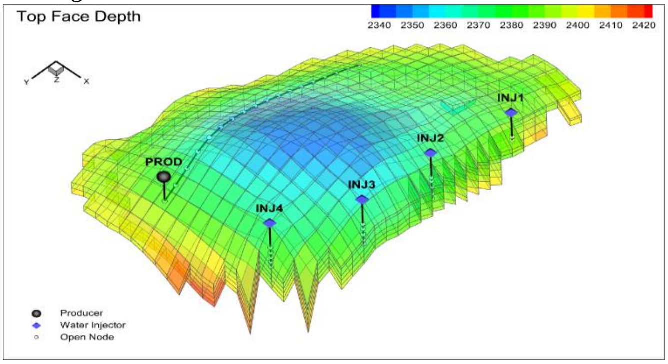


Figure 3: Production pipe and injectors topology.

Table 2 shows the rock and fluid properties of the reservoir for the simulation cases and Fig. 4 shows the porosity and permeability in different directions.

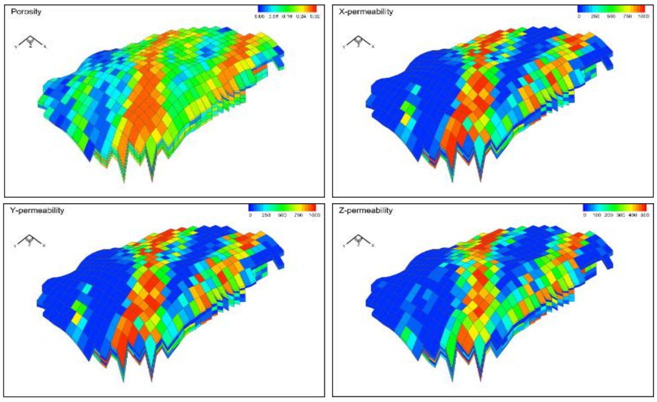


Figure 4: Porosity and permeability.

Table 2: Rock and fluid properties of the PUNQ-S3 reservoir

| **Parameter** | **Value** |
|---|---|
| Oil density | 912 $kg/m^3$ |
| Water density | 1000 $kg/m^3$ |
| Gas density | 0.8266 $kg/m^3$ |
| GOR | 74 $Sm^3$/ $Sm^3$ |
| Reservoir pressure | 234.5 bar |
| Temperature | 105 $^0$C |
| Water viscosity (reservoir condition) | 0.5 cP |
| Oil viscosity (reservoir condition) | 1.46 cP |
| Gas viscosity (reservoir condition) | 0.0133 cP |
| Porosity | 0.1 – 0.3 |
| Mean porosity | 0.14 |
| Rock compressibility | 0.000451/bar |

## 4. WELL MODEL IN OLGA

For the advanced horizontal well model, the length is specified as 3240 m in OLGA. The wellbore and production pipe have a diameter of 0.2159 m and 0.1397 m respectively. The production well has 18 valves to divide the production pipe into 18 zones. Each zone is 180 m long and separated by two packers. In reality, each section is about 12 m and consists of one flow control device (FCD). For 180 m 15 FCDs are required. In this study, each FCD is considered equivalent to 15 real FCDs. The equivalent diameter is taken as 0.0078 m for both ICD and AICD considering the discharge coefficient (CD) as 0.85. Fig. 5 shows a simplified sketch of a single production zone in a production pipe containing packers, a fluid flow path, and an inflow control device. Packers prevent fluid flow from an adjacent zone through the annulus. Near-well source is the connecting component between OLGA and ECLIPSE. Through section I fluid enters into the wellbore and then passes through the inflow control devices. After that fluid passes through the Leak into the production pipe in section II. This method was proposed by Haavard Akre in 2012 and is much used in simulation studies (Moradi and Moldestad, 2020).

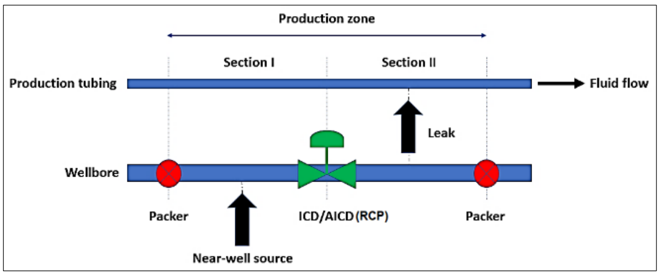


Figure 5: Schematic of a single zone in a production pipe (Moradi and Moldestad, 2020).

## 5. ALGEBRAIC CONTROLLER

The algebraic controller is a feature of OLGA for implementing algebraic equations or logical expressions to manipulate input signals for a desired output. In this study, the algebraic controller is used to control the valve opening of AICD. A mathematical equation is derived as the input signal for the AICD valve considering the oil, water, and gas volume fractions.

For ICD the pressure differential and flow rate can be written as:

$$\Delta P_{ICD} = \acute{C}_u \frac{\rho_{mix}\dot{Q}^2{}_{ICD}}{2\gamma^2 A^2 C^2{}_D}, \qquad (6)$$

$$\dot{Q}_{ICD} = \gamma A C_D \sqrt{\frac{2\Delta P_{ICD}}{\rho_{mix}\acute{C}_u}}, \qquad (7)$$

The pressure differential was derived from the available experimental data in (Halvorsen Martin et al., 2016) for AICD in the PUNQ-S3 reservoir model with similar fluid properties. Both linear and non-linear regression method was used to develop the mathematical model which is expressed by:

$$\Delta P_{AICD} = a_{AICD}\cdot\frac{\rho^2{}_{mix}}{1000}\cdot\left(\frac{1}{\mu_{mix}}\right)^y\cdot\dot{Q}^x{}_{AICD}, \qquad (8)$$

For AICD flow rate can be expressed by:

$$\dot{Q}_{AICD} = \left(\frac{1000\cdot\Delta P_{AICD}\cdot\mu^y{}_{mix}}{a_{AICD}\cdot\rho^2{}_{mix}}\right)^{\frac{1}{x}}, \qquad (9)$$

Here $\dot{Q}$ is the volumetric flow rate, $\Delta P$ is the pressure drops, $A$ is the cross-sectional area of the fluid flow, $C_D$ is the discharge coefficient, $\acute{C}_u$ is the unit conversion value, and $\gamma$ is the valve opening. Three-phase fluid mixture density and viscosity can be written as (4) and (5).

$\alpha_{oil}$, $\alpha_{water}$, $\alpha_{gas}$ are the volume fractions of oil, water, and gas in the mixture and the sum of the fractions is:

$\alpha_{oil} + \alpha_{water} + \alpha_{gas} = 1$

Now, matching $\Delta P - \dot{Q}$ curves of ICD and AICD at $\Delta P_{match}$ and $\dot{Q}_{match}$ it can be assumed that

$\Delta P_{ICD} = \Delta P_{AICD} = \Delta P_{mix}$ and $\dot{Q}_{ICD} = \dot{Q}_{AICD}$

Considering $\dot{Q}_{ICD} = \dot{Q}_{AICD}$ the valve opening can be expressed as:

$$\gamma = \frac{\left(\frac{1000.\Delta P_{mix}}{a_{AICD}}\right)^{\frac{1}{x}}}{AC_D\sqrt{\frac{2\Delta P_{mix}}{\acute{C}_u}}}\cdot\mu^{\frac{y}{x}}{}_{mix}\cdot\rho^{\frac{x-4}{2x}}{}_{mix}, \qquad (10)$$

Alternately it can be expressed as:

$$\gamma = \beta.\{\alpha_{oil}\mu_{oil} + \alpha_{water}\mu_{water} + \alpha_{gas}\mu_{gas}\}^{\frac{y}{x}}\cdot \{\alpha_{oil}\rho_{oil} + \alpha_{water}\rho_{water} + \alpha_{gas}\rho_{gas}\}^{\frac{x-4}{2x}}, \qquad (11)$$

where

$$\beta = \frac{\left(\frac{1000.\Delta P_{mix}}{a_{AICD}}\right)^{\frac{1}{x}}}{AC_D\sqrt{\frac{2\Delta P_{mix}}{\acute{C}_u}}}, \qquad (12)$$

and

$$\{\alpha_{oil}\mu_{oil} + \alpha_{water}\mu_{water} + \alpha_{gas}\mu_{gas}\}^{\frac{y}{x}} = \mu^{\frac{y}{x}}{}_{mix}$$
$$\{\alpha_{oil}\rho_{oil} + \alpha_{water}\rho_{water} + \alpha_{gas}\rho_{gas}\}^{\frac{x-4}{2x}} = \rho^{\frac{x-4}{2x}}{}_{mix}, \qquad (13)$$

In the OLGA model, two transmitters are used to take the values of the volume fraction of oil ($\alpha_{oil}$) and water ($\alpha_{water}$) as an input variable from the wellbore. Equation (8) is put as an expression option in the algebraic controller in OLGA. To implement $\alpha_{oil}$, $\alpha_{water}$ as input variables into (14), they are introduced as unknown variables X1 and X2 in the algebraic controller. The expression in the algebraic controller is as follows:

$$\gamma = \beta.\{X1\cdot\mu_{oil} + X2\cdot\mu_{water} + (1 - X1 - X2)\cdot\mu_{gas}\}^{\frac{y}{x}}\cdot \{X1\cdot\rho_{oil} + X2\cdot\rho_{water} + (1 - X1 - X2)\cdot\rho_{gas}\}^{\frac{x-4}{2x}}, \qquad (14)$$

Here $\alpha_{oil} = X1$, $\alpha_{water} = X2$ and $\alpha_{gas} = 1 - X1 - X2$

Experimental data were used to find the parameters in (12) using multivariable nonlinear regression. The values in Appendix A are based on that. Fig. 6 shows the controller behavior as the valve opening control for AICD according to different phases of the fluids.

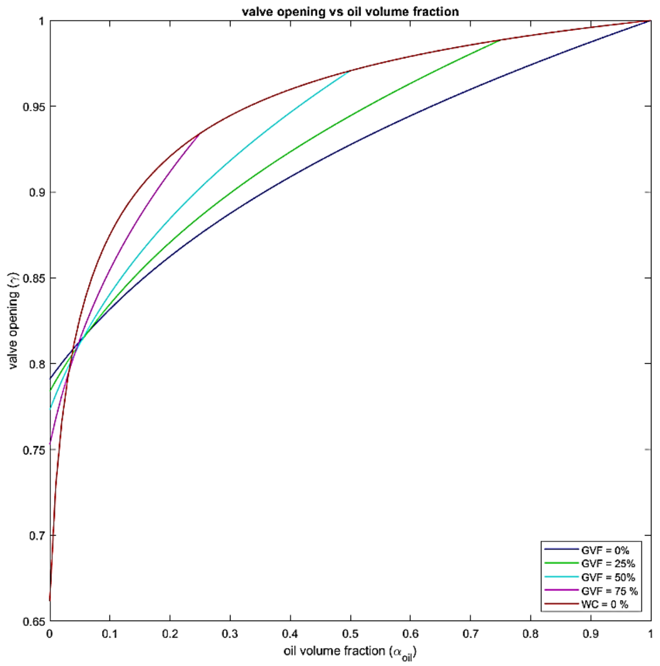


Figure 6: Valve opening vs oil volume fraction for the algebraic controller in different phases of fluid.

## 6. RESULTS AND DISCUSSION

In this chapter, the obtained simulation results from the OLGA/ECLIPSE model are shown and discussed. Performance analysis of ICD and AICD are shown and compared to the OPENHOLE case for improving oil recovery and reducing water cut. The functionality of the algebraic controller controlling the valve opening of AICD is analyzed considering water cut and gas volume fraction (GVF). The pressure drop for the cases was considered 15 bar with a constrained liquid production rate of 4000m$^3$/day for ICD.

### *6.1 Total oil and water production*

The total flow of oil and water are two of the most important parameters to analyze for the performance of the FCDs. Fig. 7 illustrates the total oil and water production for OPENHOLE and FCDs. OPENHOLE has a larger cross-sectional inlet area and there are no restrictions for liquid production so more water and oil can be produced compared to FCDs. ICD and AICD had the same amount of oil production, and both of the curves overlapped (blue over black), and this can happen because of the recovery of low viscous oil. The functionality of AICD can be observed with higher oil production if the simulation time was more than 3500 days. It is very important to have less water production for a better economy and environmental impact. In this case, FCDs showed better performance producing less water than OPENHOLE. In the cases of ICD and AICD, the water production is reduced by 33.8% and 36.3% respectively compared to the OPENHOLE case. The AICD reduced the accumulated water production by 3.7% compared to the ICD. This indicates that AICD has a better choking effect on low viscous fluid like water. Less water production means less production cost in the oil processing step after recovery.

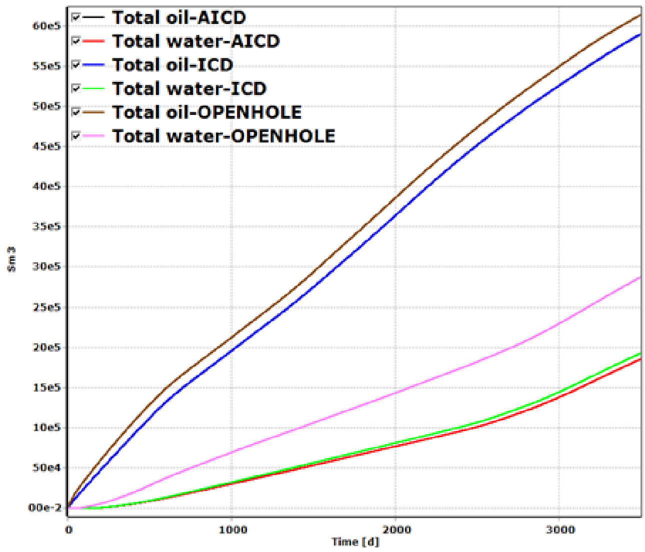


Figure 7: Total oil and water production.

### *6.2 Oil and water production rate*

OPENHOLE has a larger cross-sectional area to produce more liquid than FCDs. Fig. 8 illustrates the oil and water production rate for 3500 days of simulation.

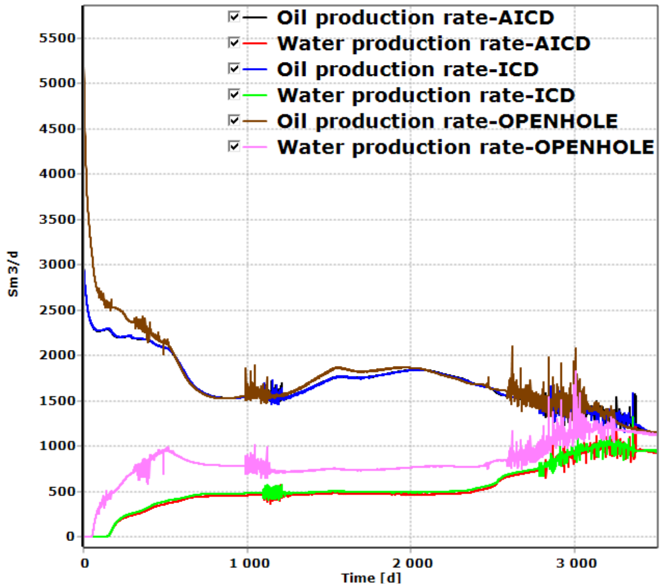


Figure 8: Oil and water production rate.

The OPENHOLE case has a larger cross-sectional area which is exposed to production. For this reason, OPENHOLE has a higher fluid production rate. In reality, there is a limitation for maximum fluid production with a regulating valve on topside, but this is not considered for this study. After 1000 days the oil production rate increased because of gas injection. It can be observed that after 3500 days FCDs are showing a tendency to produce more oil than OPENHOLE. So, simulation for more than 3500 days can result in a higher oil production rate for the FCDs. ICD and AICD almost have the exact amount of oil showing the blue curve overlapping over the black curve. But ICD has a higher production rate of water than AICD. This is because ICDs cannot prevent further production after the water enters the well whereas AICD is partially closed when water enters through the inlet. This also proves the choking ability of AICD to the low viscous fluids.

### *6.3 Algebraic controller behavior to WC*

In this study algebraic controller is used to control the valve opening of the AICD. Equation (12) was implemented by expression form in the algebraic controller. Fig. 9 shows the valve opening control according to the WC. A total of 18 controllers were used in the well model. Among those, controller 1 and controller 18 are chosen for the toe and heel respectively. A maximum water cut of 0.64 and 0.82 was found for the toe and heel sections. At the toe section, the minimum valve opening was 90% fully open and at the heel section, the minimum valve opening was 85%. It can be observed that the more the water cut increased the more the valve was closing. From this observation, it can be said that the algebraic controller is showing the choking effect on water production.

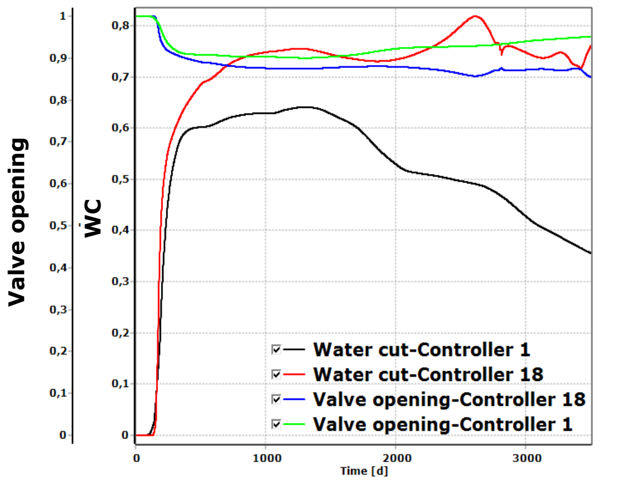


Figure 9: Valve opening with algebraic controller in toe and heel section for water cut.

### *6.4 Algebraic controller behavior to GVF*

To observe the functionality of valve opening of the algebraic controller according to the GVF, controllers 8 and 9 at the middle of the horizontal well were selected. Fig. 10 shows the behavior of the algebraic controller for the GVF.

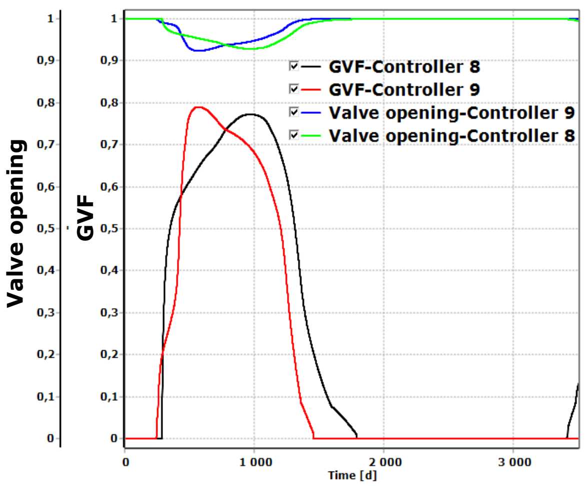


Figure 10: Valve opening of the algebraic controller according to GVF.

A maximum GVF of 0.77 and 0.79 was found for the controllers 8 and 9 respectively. For controller 8 the valve opening was up to 0.93 and for controller 9 valve opening was up to 0.92. It can be observed that the more the GVF increased the more the valve was getting closed. From this observation, it can be said that the algebraic controller is showing the choking effect on gas volume fraction.

## 7. CONCLUSIONS

According to the findings from the simulations, it can be concluded that FCDs show a better impact on the WAG injection oil recovery process in heterogeneous reservoir. ICD and AICD have reduced water production by 33.8% and 36.3% respectively compared to OPENHOLE. The most important part of this study was to implement and investigate the performance of the algebraic controller in terms of controlling the valve opening of AICD. Though the oil production rate was the same for both ICD and AICD, water production was 3.7%. lower for AICD compared to ICD. This satisfies the main purpose of using AICD to minimize water production. It also indicates the performance of the algebraic controller that can be implemented for AICD valve opening in the OLGA simulator. It showed better performance in controlling valve opening with increasing WC and GVF. Using the transmitters for getting input of oil and water volume fractions to the controller and manipulating the valve opening from a logical mathematical expression was also successful.

## ACKNOWLEDGEMENT


We gratefully acknowledge the economic support from the Research Council of Norway and Equinor through Research Council Project No. 308817, “Digital Wells for Optimal Production and Drainage” (DigiWell).


## REFERENCES


Al-Khelaiwi, F.T., D.R., D. (2007). Inflow Control Devices: Application and Value Quantification of a Developing Technology. International Oil Conference and Exhibition. https://doi.org/https://doi.org/10.2118/108700-MS

Birchenko, V.M., Muradov, K.M., Davies, D.R. (2010). Reduction of the horizontal well’s heel-toe effect with inflow control devices. J Pet Sci Eng 75, 244–250. https://doi.org/10.1016/j.petrol.2010.11.013

Halvorsen Martin, Madsen Martin, Vikøren Mo Mathias, Isma Mohd Ismail, Green Annabel (2016). Enhanced Oil Recovery On Troll Field By Implementing Autonomous Inflow Control Device . Annabel . https://doi.org/https://doi.org/10.2118/180037-MS

Hutahaean, J.J.J. (2017). Multi-Objective Methods for History Matching, Uncertainty Prediction and Optimisation in Reservoir Modelling. Heriot-Watt University.

Mathiesen, V., Aakre, H., Werswick, B., Elseth, G. (2011). The Autonomous RCP Valve-New Technology for Inflow Control In Horizontal Wells, in: SPE Offshore Europe Oil and Gas Conference and Exhibition. Aberdeen, UK. https://doi.org/https://doi.org/10.2118/145737-MS

Moradi, A., Moldestad, B.M.E. (2020). Near-well simulation of oil production from a horizontal well with ICD and AICD completions in the Johan Sverdrup field using OLGA/ROCX, in: Proceedings of The 61st SIMS Conference on Simulation and Modelling SIMS 2020, September 22-24, Virtual Conference, Finland. Linköping University Electronic Press, pp. 249–256. https://doi.org/10.3384/ecp20176249

Appendix A

| **Parameter** | **Value** |
|---|---|
| $C_D$ | 0.85 |
| $\acute{C}_u$ | $1.34 \cdot e^{-15}$ |
| $a_{AICD}$ | $3.41 \cdot e^{-6}$ |
| $\Delta P_{mix}$ | 20 bar |
| $A = \frac{\pi}{4} D^2$ | $\frac{\pi}{4}(0.002)^2 = 3.2687 \cdot e^{-5}$ |
| $x$ | 3.35 |
| $y$ | 0.4 |
| $\mu_{oil}$ | 2.7 |
| $\mu_{water}$ | 0.45 |
| $\mu_{gas}$ | 0.02 |
| $\rho_{oil}$ | 890 kg/m$^3$ |
| $\rho_{water}$ | 1100 kg/m$^3$ |
| $\mu_{gas}$ | 150 kg/m$^3$ |